


Scattering laser light from two resonant quantum dots in a photonic crystal waveguide

Joel Q. Grim^{1,*}, Ian Welland,² Samuel G. Carter,¹ Allan S. Bracker,¹ Andrew Yeats¹, Chul Soo Kim¹, Mijin Kim³,
Kha Tran,² Igor Vurgaftman¹ and Thomas L. Reinecke¹

¹Naval Research Laboratory, 4555 Overlook Avenue SW, Washington, DC 20375, USA

²NRC Research Associate at the Naval Research Laboratory, 4555 Overlook Avenue SW, Washington, DC 20375, USA

³Jacobs, Hanover, Maryland 21076, USA

 (Received 15 November 2021; revised 15 July 2022; accepted 2 August 2022; published 15 August 2022)

We demonstrate the scattering of laser light from two InAs quantum dots coupled to a photonic crystal waveguide, which is achieved by strain-tuning the optical transitions of the dots into mutual resonance. By performing measurements of the intensity and photon statistics of transmitted laser light before and after tuning the dots into resonance, we show that the nonlinearity is enhanced by scattering laser light from two dots. In addition to providing a means of manipulating few-photon optical nonlinearities, our approach establishes opportunities for multiemitter quantum optics in a solid-state platform.

DOI: [10.1103/PhysRevB.106.L081403](https://doi.org/10.1103/PhysRevB.106.L081403)

An efficient photon-photon nonlinearity is a key resource that is needed to access and to use quantum information stored in light [1,2], thus underpinning the operation of components such as single-photon switches and all-optical deterministic quantum logic gates [3–5]. An appealing approach to produce such a nonlinearity is with a coherent light-matter interface of quantum emitters such as atoms [6,7] or solid-state “artificial atoms” [8–12] coupled to a single-mode nanophotonic waveguide (WG). Operated as two-level systems, these emitters can be saturated by the single-photon component of a resonant coherent input field, producing a giant optical nonlinearity at the quantum limit. This giant nonlinearity has recently been demonstrated by scattering weak coherent laser light from single semiconductor quantum dots (QDs) embedded in photonic crystal (PhC) WGs [8,9,11]. In this approach, a QD can manipulate the classical coherent input to generate a nonclassical output, including exotic states of light such as energy-time entangled two-photon bound states [8,9,11,13]. Waveguide quantum electrodynamics also offers a tantalizing platform for realizing multibody quantum optics, with dispersion and modal engineering possibilities that are inaccessible to traditional cavity QED. This has generated significant recent theoretical and experimental interest from solid-state [10,14–18], atomic [6,14,19], and superconducting qubit communities [20].

Scattering resonant laser light from multiple emitters could provide new opportunities for quantum information processing components such as single-photon switches and all-optical deterministic quantum logic gates [3–5], but it remains challenging for atomic systems and unexplored for QDs. For atomic systems, despite progress in creating deterministic atom-WG interfaces [21], it is difficult to efficiently couple atoms to WGs. It has been shown that this can be overcome by scattering from an ensemble of atoms weakly coupled to a

waveguide, resulting in a collective enhancement of correlated photon pairs [6]. On the other hand, strong and deterministic WG coupling is routinely achieved with solid-state emitters such as QDs [8,9,11] and defects in diamond [10,15], but the variation in optical transition frequencies of solid-state emitters has made the demonstration of multiemitter quantum optics an ongoing challenge. Although there has been recent progress in demonstrating collective quantum phenomena such as superradiance through the emission of indistinguishable photons from multiple solid-state emitters coupled to the same WG mode [10,14–18], scattering resonant laser light from multiple QDs has not yet been demonstrated.

In this Letter, we demonstrate collective scattering of laser light from two QDs coupled to a single mode PhC WG. This result is made possible by a strain-tuning technique that we recently developed [16], which allows the optical transitions of multiple QDs to be tuned into mutual resonance within the same PhC WG. For these experiments, a continuous-wave (cw) laser is transmitted through a photonic crystal WG with embedded InAs QDs. By tuning the laser on-resonance with a two-level QD optical transition, the single-photon component of the coherent laser field is reflected and correlated photon pairs (photon bound states) are transmitted [6,8,11]. The QD-WG coupling efficiency (β) is a key parameter that controls the size of the nonlinearity that can be observed in these experiments, with the magnitude of the transmission dip proportional to $1-\beta$ for a transmitted weak input field resonant with a QD. We show that collective scattering produces a larger nonlinearity in the transmitted intensity as well as in the bunching in second-order photon correlation measurements compared to individual QDs, with both effects arising from a higher probability of single photons scattering from two QDs than from one.

These concepts are illustrated schematically in Fig. 1(a) and with the calculations in Figs. 1(b) and 1(c) using the input-output formalism developed in Refs. [11,22] (see the Supplemental Material [23] for details of the model). For

*Corresponding author: joel.grim@nrl.navy.mil

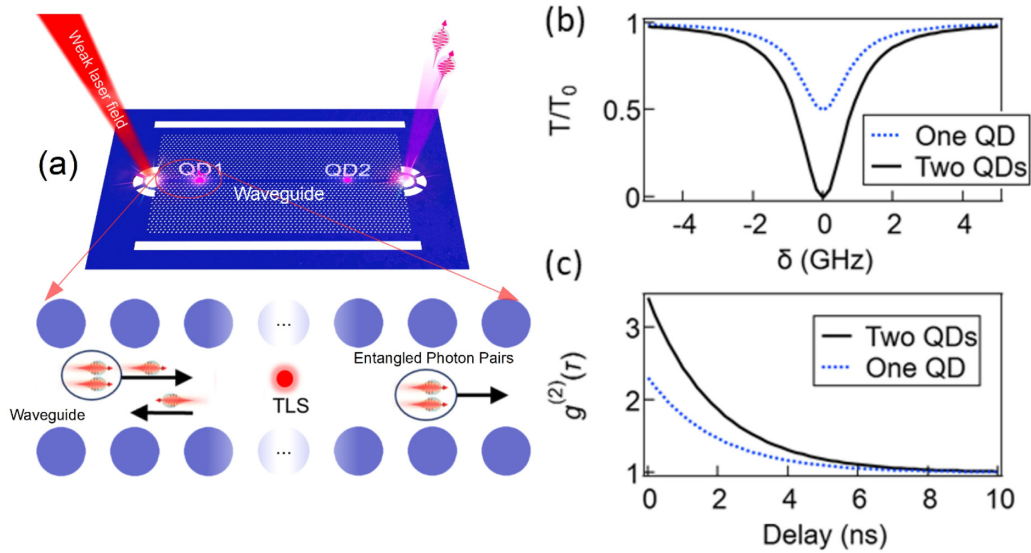


FIG. 1. (a) Photonic crystal waveguide containing embedded QDs and transmission experiment schematic. Calculated transmission (b) spectra and (c) second-order autocorrelation $g^{(2)}(\tau)$ functions for one QD and two resonant QDs for a weak coherent input field and assuming an ideal waveguide (no end-facet reflections), with $\beta = 0.5$ and $\Gamma = 1$ GHz.

a weak coherent input field and $\beta = 0.5$ for each QD, i.e., light transmitted through the waveguide has a 50% probability of scattering from each QD, as shown in Fig. 1(b). When the QDs are in resonance, the magnitude of the transmission dip $1 - T/T_0$ increases. The bunched photon statistics around $\tau = 0$ in the calculated $g^{(2)}(\tau)$ curves in Fig. 1(c) result from the preferential transmission of two-photon bound states compared to single-photon states, due to the nonlinear interaction with the QDs at the few photon level [8, 11, 24–26]. Increasing the number of QDs to 2 essentially purifies the two-photon output, resulting in a larger bunching peak for two resonant QDs.

We use InGaAs QDs grown by molecular beam epitaxy embedded in GaAs PhC membrane waveguides with a vertical $n-i-n-i-p$ heterostructure for deterministic control of the QD charge state [16]. Experiments were performed at 5.3 K with a 0.75 NA temperature-controlled objective in the vacuum space of a closed-cycle cryostat and a custom confocal μ PL (photoluminescence) set up. We use the optically active negative trion (X^-) QD charge state, which has doubly degenerate transitions from the electron spin ground states to X^- states at zero magnetic field and can therefore be treated as a two-level system. The QDs are strain-tuned into resonance using a technique in which an above-gap laser is used to locally crystallize a thin HfO_2 film on the surface of the PhC membrane, allowing multiple QDs embedded in the same PhC WG to be brought into mutual resonance [16]. The spatial positions of the QDs (labeled QD1 and QD2 throughout) were determined using an optical image of the sample and by scanning an above-gap laser over the waveguide while monitoring the PL. From this, we determine a QD1-QD2 distance of $4 \pm 0.3 \mu\text{m}$.

We first characterize the photon statistics of the X^- PL from two QDs excited by a 1353 meV nonresonant cw laser through the PhC WG mode, as shown in Fig. 2. We note that these $g^{(2)}(\tau)$ measurements of QD PL demonstrate the single- and indistinguishable-photon emission properties of the dots

that were used for the laser scattering experiments shown in Figs. 3 and 4 and also serve as a comparison to previous work (Refs. [10, 15–17]). In Fig. 2, we show the measured second-order autocorrelation function $g^{(2)}(\tau)$ using a Hanbury Brown-Twiss setup for three regimes in Fig. 2: (i) single-photon emission from one QD, (ii) distinguishable emission from two nonresonant QDs, (iii) and indistinguishable emission from two resonant QDs. The single-photon emission was measured by sending the emission from QD2 through a narrow-band filter, resulting in antibunched $g^{(2)}(0) \approx 0.084$ statistics (black points in Fig. 2). After tuning QD1 to within $50 \mu\text{eV}$ of QD2, the emission from both QDs was sent through the same filter with $g^{(2)}(0) \approx 0.6$ (blue points in Fig. 2), as expected for two distinguishable photon sources [16]. The small

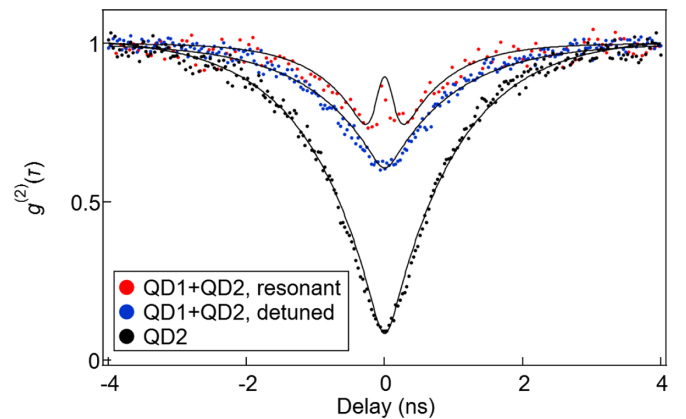


FIG. 2. Second-order autocorrelation measurements of the PL from (i) one QD (black dots), (ii) two distinguishable QDs (blue dots), and (iii) two indistinguishable QDs (red dots) excited by nonresonant 1353-meV laser light. $g^{(2)}(0) \rightarrow 0$ for one QD (QD2), $g^{(2)}(0) \rightarrow 0.5$ collecting emission from both QD1 and QD2 when they are detuned from one another, and $g^{(2)}(0) \rightarrow 1$ when QD1 and QD2 are resonant due to the quantum interference of indistinguishable photons in the waveguide [15–17, 27].

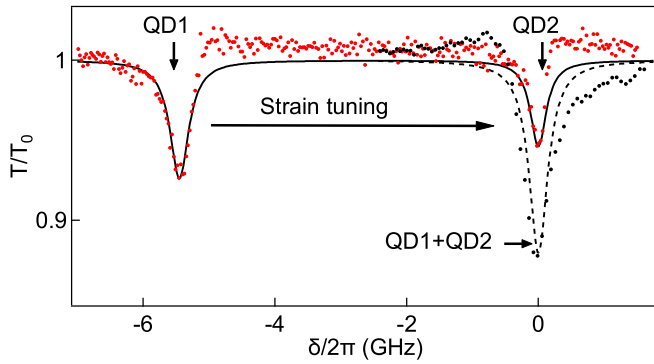


FIG. 3. The measured negative trion (X^-) transmission for QD1 and QD2 as a function of detuning $\delta/2\pi$ from the excitation laser is shown prior to (red points) as well as after strain-tuning QD1 into resonance with QD2 (black points). The parameters determined from fits to QD1 and QD2 (black line) were used to calculate the resonant QD spectrum (black dashed line), without including the Fano effect, which is extraneous to the process of interest and does not affect the value of the linewidths that are determined.

discrepancy of the experimental data from the theoretical values of $g^{(2)}(0) = 0$ and 0.5 , respectively, is predominantly due to background PL excited by the nonresonant laser. After tuning QD1 and QD2 into resonance, a bunching peak emerges with $g^{(2)}(0) = 0.86$ (red points in Fig. 2) due to the quantum interference of indistinguishable photons emitted by both QDs and is one signature of superradiance [15–17,27]. The difference from the theoretical value of $g^{(2)}(0) = 1$ is due to a small spectral detuning between the QDs caused by the relatively high power of $2 \mu\text{W}$ used for the nonresonant 1353-meV excitation laser. We emphasize that Figs. 2 and 4(b) display photon statistics that originate from different physical mechanisms. The former shows measurements of the photoexcited emission from the dots, and the latter shows measurements of transmitted laser light that resonantly scatters from the dots.

Next, we show laser scattering from the same two QDs. The laser transmission experiments are performed by transmitting a weak, tunable cw laser through the WG. In Fig. 3, the normalized transmission intensity T/T_0 is shown as a function of laser detuning (plotted relative to QD2) with QD1 and QD2 in the X^- charge state. T_0 is the transmission intensity of the bare WG measured at an electrical bias far-detuned from the X^- charge state, where the quantum dots do not absorb. The spectrum is shown before (red points) and after (black points) tuning QD1 into resonance with QD2, with transition linewidths of 0.48 and 0.27 GHz for QD1 and QD2, respectively. The asymmetric line shapes originate from Fano interference caused by reflections from the PhC WG end facets that produce Fabry-Pérot modes [8,11], and depend on the detuning from these modes (see the Supplemental Material [23] for the PhC WG transmission spectrum).

We use the formalism of Ref. [28] for coupled two-level emitters to model the spectra in Fig. 3. We account for spectral diffusion by running this calculation repeatedly with the spectral positions of each dot taken randomly and independently from a Gaussian distribution and averaging the results. Using the radiative emission rate $\gamma_R/2\pi = 0.16$ GHz for

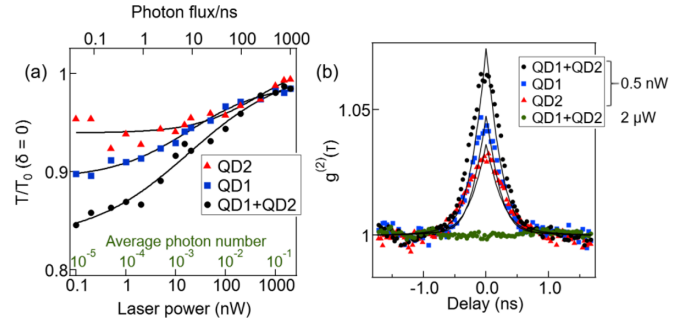


FIG. 4. Nonlinearity of resonant and nonresonant QDs in a waveguide as a function of transmitted laser power. (a) Saturation of transmission intensity on resonance for QD1, QD2, and QD1 + QD2 versus laser power (measured before the objective) under the spectral conditions shown in Fig. 3. The average photon number in the waveguide vs power is shown with the green axis (after accounting for coupling losses). (b) Second-order autocorrelation function measurements of an on-resonant transmitted laser with a power of 0.5 nW before the objective. The bunching around zero delay [$g^{(2)}(0) > 1$] for QD1 (blue squares), QD2 (red triangles), and QD1 and QD2 in resonance (black circles) is due to the preferential transmission of two-photon bound states. The black lines are $g^{(2)}(\tau)$ calculations using parameters obtained from fitting the transmission spectra in Fig. 3. At high power ($2 \mu\text{W}$) above the saturation of the QDs, the Poissonian statistics of the input coherent laser field results in $g^{(2)}(0) = 1$, shown with green points.

both QD1 and QD2 determined from the measured $g^{(2)}(\tau)$ under nonresonant excitation (see Fig. 2), fits to the detuned QD1 and QD2 spectra in Fig. 3 yield the following parameters: $\beta_{\text{QD1}} = 0.14$, $\beta_{\text{QD2}} = 0.075$, and $\sigma_{\text{SD, QD1}} = 0.12$ GHz, $\sigma_{\text{SD, QD2}} = 0.065$ GHz, where σ_{SD} is the broadening due to spectral diffusion. We use these parameters to calculate the transmission spectrum for zero detuning between the dots, and find excellent agreement with the two-dot experimental data (black points) for the magnitude of the transmission dip, as shown with the black dashed curve in Fig. 3. Further, the predicted increase in the width of the transmission dip for two dots in this model is due to an increased emission rate into the WG due to superradiance [28], which agrees very well with the measured linewidth of 0.64 GHz for the resonant dots. However, while the superradiant emission rate enhancement does not significantly change the magnitude of the predicted transmission dip, it does increase the bandwidth. For simplicity, we do not include the Fano effect in this model, but note that the change in the asymmetric line shape before and after strain tuning is due to a shift in the WG spectrum caused by the removal of condensed nitrogen from the PhC membrane due to laser heating. Including a Fano parameter does not change the value of the linewidths that are determined.

We next demonstrate the nonlinearity of this system for individual and collective coherent scattering from QD1 and QD2. The following experiments were performed under the spectral conditions shown in Fig. 3. A cw laser was tuned on-resonance with each transition, and the transmitted power-dependent behavior is examined, providing a characteristic measure of saturation nonlinearity. Figure 4(a) plots the depth of the laser transmission dip for QD1 (blue squares), QD2 (red triangles), and QD1 and QD2 in resonance (black points)

as a function of on-resonant laser power (measured before the objective). The average number of photons in the waveguide at the same time is shown with the green axis, and is determined from the white light WG transmission spectrum (see the Supplemental Material [23]). In each case, the magnitude of the transmission dip ($1-T/T_0$) decreases with increasing laser power due to saturation of the QDs, and the dots eventually become transparent to the incoming field at high power ($>1 \mu\text{W}$). This change in transmission intensity versus laser power is larger for resonant QDs [QD1 + QD2 in Fig. 4(a)] due to the increased probability of laser light scattering from two dots compared to one.

Insight into the quantum nature of this nonlinearity is gained from measuring the photon statistics of the transmitted laser. Figure 4(b) plots $g^{(2)}(\tau)$ for detuned individual QDs and for both QDs in resonance, all with $g^{(2)}(\tau=0) > 1$ bunching, which originates from a greater probability of two photons being transmitted through the QDs compared to one photon [8,9,11]. The two-level QDs act to partially filter out single-photon states. With the QDs in resonance, the bunching peak is larger, which is due to a greater probability of filtering single photons due to collective scattering. We calculate $g^{(2)}(\tau)$ using the input-output formalism developed in Refs. [11,22] [black lines in Fig. 4(b)] and the parameters obtained from fitting the transmission spectra shown in Fig. 3 (see the Supplemental Material [23]). At high power, the QDs are effectively transparent due to saturation and the transmitted laser displays Poisson statistics, as shown in Fig. 4(b) for a laser power of $2 \mu\text{W}$. In the Supplemental Material [23], we show additional examples of collective scattering from QDs with weaker coupling (lower β) as well as stronger (higher β) coupling efficiency to WGs. The same general features are observed, including an enhanced nonlinearity beyond the performance of the individual QDs, and a nonlinearity down to the single-photon level is observed for QDs with stronger coupling to the WG.

Although the distance between dots was different in each of our examples and was not preselected, an important consideration is whether it has any effect on these experiments. For example, particular distances can result in cavitylike behavior with the QDs acting as quantum mirrors, which can produce a narrow transparency window in the transmission spectrum [20,28]. However, in addition to requiring near-unity QD-WG coupling, the spectral diffusion of the QDs used in this work makes the observation of this effect unlikely. Such observations may become possible with further advances in precise positioning of the QDs through site-controlled growth [29] within PhC membranes as well as the use of QDs with near-unity WG coupling [30] and transform-limited linewidths [31]. By extending this technique beyond two QDs and with somewhat better coupling to the WG, we expect that the transmission dip can go down much closer to zero, providing a highly nonlinear element at the single-photon level.

This Letter demonstrates scattering resonant laser light from pairs of QDs coupled to PhC WGs, an achievement that opens opportunities for exploring the few-emitter regime that has been challenging to realize for both solid-state and atomic systems. This enables a systematic study of multi-emitter quantum optics and establishes the potential of this platform for realizing proposals of many-body states of light [32,33]. The manipulation of quantum optical nonlinearities that has been made possible with this work has the potential to impact the creation of single-photon switches and all-optical deterministic quantum logic gates [3–5], the study of non-Markovian effects [34], and the formation of subradiant states for long-lived quantum memories [27], and open possibilities for the study and control of multiphoton dark states [20].

This work was supported by the U.S. Office of Naval Research. I.W. and K.T. are NRC Research Associates at the U.S. Naval Research Laboratory.

-
- [1] A. J. Bennett, J. P. Lee, D. J. P. Ellis, I. Farrer, D. A. Ritchie, and A. J. Shields, A semiconductor photon-sorter, *Nat. Nanotechnol.* **11**, 857 (2016).
 - [2] T. Peyronel, O. Firstenberg, Q. Y. Liang, S. Hofferberth, A. V. Gorshkov, T. Pohl, M. D. Lukin, and V. Vuletić, Quantum nonlinear optics with single photons enabled by strongly interacting atoms, *Nature (London)* **488**, 57 (2012).
 - [3] E. Shahmoon, G. Kurizki, M. Fleischhauer, and D. Petrosyan, Strongly interacting photons in hollow-core waveguides, *Phys. Rev. A* **83**, 033806 (2011).
 - [4] D. Solenov, S. E. Economou, and T. L. Reinecke, Fast two-qubit gates for quantum computing in semiconductor quantum dots using a photonic microcavity, *Phys. Rev. B* **87**, 035308 (2013).
 - [5] A. V. Gorshkov, J. Otterbach, M. Fleischhauer, T. Pohl, and M. D. Lukin, Photon-Photon Interactions Via Rydberg Blockade, *Phys. Rev. Lett.* **107**, 133602 (2011).
 - [6] A. S. Prasad, J. Hinney, S. Mahmoodian, K. Hammerer, S. Rind, P. Schneeweiss, A. S. Sørensen, J. Volz, and A. Rauschenbeutel, Correlating photons using the collective non-linear response of atoms weakly coupled to an optical mode, *Nat. Photonics* **14**, 719 (2020).
 - [7] M. Bajcsy, S. Hofferberth, V. Balic, T. Peyronel, M. Hafezi, A. S. Zibrov, V. Vuletic, and M. D. Lukin, Efficient All-Optical Switching Using Slow Light within a Hollow Fiber, *Phys. Rev. Lett.* **102**, 203902 (2009).
 - [8] A. P. Foster, D. Hallett, I. V. Iorsh, S. J. Sheldon, M. R. Godland, B. Royall, E. Clarke, I. A. Shelykh, A. M. Fox, M. S. Skolnick, I. E. Itskevich, and L. R. Wilson, Tunable Photon Statistics Exploiting the Fano Effect in a Waveguide, *Phys. Rev. Lett.* **122**, 173603 (2019).
 - [9] A. Javadi, I. Söllner, M. Arcari, S. Lindskov Hansen, L. Midolo, S. Mahmoodian, G. Kiršanskė, T. Pregolato, E. H. Lee, J. D. Song, S. Stobbe, and P. Lodahl, Single-Photon non-linear optics with a quantum dot in a waveguide, *Nat. Commun.* **6**, 6 (2015).
 - [10] A. Sipahigil, R. E. Evans, D. D. Sukachev, M. J. Burek, J. Borregaard, M. K. Bhaskar, C. T. Nguyen, J. L. Pacheco, H. A. Atikian, C. Meuwly, R. M. Camacho, F. Jelezko, E. Bielejec, H. Park, M. Lončar, and M. D. Lukin, An integrated diamond

- nanophotonics platform for quantum optical networks, *Science* **354**, 847 (2016).
- [11] H. Le Jeannic, T. Ramos, S. F. Simonsen, T. Pregolato, Z. Liu, R. Schott, A. D. Wieck, A. Ludwig, N. Rotenberg, J. J. García-Ripoll, and P. Lodahl, Experimental Reconstruction of the Few-Photon Nonlinear Scattering Matrix from a Single Quantum Dot in a Nanophotonic Waveguide, *Phys. Rev. Lett.* **126**, 023603 (2021).
- [12] A. Auffèves-Garnier, C. Simon, J. M. Gérard, and J. P. Poizat, Giant optical nonlinearity induced by a single two-level system interacting with a cavity in the purcell regime, *Phys. Rev. A* **75**, 053823 (2007).
- [13] J. T. Shen and S. Fan, Strongly Correlated Two-Photon Transport in a One-Dimensional Waveguide Coupled to a Two-Level System, *Phys. Rev. Lett.* **98**, 153003 (2007).
- [14] A. Goban, C. L. Hung, J. D. Hood, S. P. Yu, J. A. Muniz, O. Painter, and H. J. Kimble, Superradiance for Atoms Trapped Along a Photonic Crystal Waveguide, *Phys. Rev. Lett.* **115**, 063601 (2015).
- [15] B. Machielse, S. Bogdanovic, S. Meesala, S. Gauthier, M. J. Burek, G. Joe, M. Chalupnik, Y. I. Sohn, J. Holzgrafe, R. E. Evans, C. Chia, H. Atikian, M. K. Bhaskar, D. D. Sukachev, L. Shao, S. Maity, M. D. Lukin, and M. Lončar, Quantum Interference of Electromechanically Stabilized Emitters in Nanophotonic Devices, *Phys. Rev. X* **9**, 031022 (2019).
- [16] J. Q. Grim, M. Zalalutdinov, S. G. Carter, A. C. Kozen, M. Kim, C. S. Kim, J. T. Mlack, M. Yakes, B. Lee, and D. Gammon, Scalable in operando strain tuning in nanophotonic waveguides enabling three-quantum-dot superradiance, *Nat. Mater.* **18**, 963 (2019).
- [17] J. H. Kim, S. Aghaieimibodi, C. J. K. Richardson, R. P. Leavitt, and E. Waks, Super-Radiant emission from quantum dots in a nanophotonic waveguide, *Nano Lett.* **18**, 4734 (2018).
- [18] J. S. Douglas, H. Habibiyan, C. L. Hung, A. V. Gorshkov, H. J. Kimble, and D. E. Chang, Quantum many-body models with cold atoms coupled to photonic crystals, *Nat. Photonics* **9**, 326 (2015).
- [19] S. Mahmoodian, M. Čepulkovskis, S. Das, P. Lodahl, K. Hammerer, and A. S. Sørensen, Strongly Correlated Photon Transport in Waveguide Quantum Electrodynamics with Weakly Coupled Emitters, *Phys. Rev. Lett.* **121**, 143601 (2018).
- [20] M. Mirhosseini, E. Kim, X. Zhang, A. Sipahigil, P. B. Dieterle, A. J. Keller, A. Asenjo-Garcia, D. E. Chang, and O. Painter, Cavity quantum electrodynamics with Atom-like mirrors, *Nature (London)* **569**, 692 (2019).
- [21] A. Goban, C.-L. Hung, S.-P. Yu, J. D. Hood, J. A. Muniz, J. H. Lee, M. J. Martin, A. C. McClung, K. S. Choi, D. E. Chang, O. Painter, and H. J. Kimble, Atom-Light interactions in photonic crystals, *Nat. Commun.* **5**, 3808 (2014).
- [22] T. Ramos and J. J. García-Ripoll, Multiphoton Scattering Tomography with Coherent States, *Phys. Rev. Lett.* **119**, 153601 (2017).
- [23] See Supplemental Material at <http://link.aps.org/supplemental/10.1103/PhysRevB.106.L081403> for details on the model of resonant scattering from two emitters, the waveguide transmission spectrum, additional examples of laser scattering from pairs of QDs, and the sample structure and additional experimental details.
- [24] M. F. Maghrebi, M. J. Gullans, P. Bienias, S. Choi, I. Martin, O. Firstenberg, M. D. Lukin, H. P. Büchler, and A. V. Gorshkov, Coulomb Bound States of Strongly Interacting Photons, *Phys. Rev. Lett.* **115**, 123601 (2015).
- [25] D. E. Chang, A. S. Sørensen, E. A. Demler, and M. D. Lukin, a single-photon transistor using nanoscale surface plasmons, *Nat. Phys.* **3**, 807 (2007).
- [26] Q. Liang, A. V. Venkatramani, S. H. Cantu, T. L. Nicholson, M. J. Gullans, A. V. Gorshkov, J. D. Thompson, C. Chin, M. D. Lukin, and V. Vuleti, Observation of three-photon bound states in a quantum nonlinear medium, *Science* **359**, 783 (2018).
- [27] R. E. Evans, M. K. Bhaskar, D. D. Sukachev, C. T. Nguyen, A. Sipahigil, M. J. Burek, B. Machielse, G. H. Zhang, A. S. Zibrov, E. Bielejec, H. Park, M. Lončar, and M. D. Lukin, Photon-Mediated interactions between quantum emitters in a diamond nanocavity, *Science* **362**, 662 (2018).
- [28] S. Das, V. E. Elfving, F. Reiter, and A. S. Sørensen, Photon scattering from a system of multilevel quantum Emitters. II. Application to emitters coupled to a one-dimensional waveguide, *Phys. Rev. A* **97**, 043838 (2018).
- [29] M. K. Yakes, L. Yang, A. S. Bracker, T. M. Sweeney, P. Brereton, M. Kim, C. S. Kim, P. M. Vora, D. Park, S. G. Carter, and D. Gammon, Leveraging crystal anisotropy for deterministic growth of inas quantum dots with narrow optical linewidths, *Nano Lett.* **13**, 4870 (2013).
- [30] M. Arcari, I. Söllner, A. Javadi, S. Lindskov Hansen, S. Mahmoodian, J. Liu, H. Thyrrstrup, E. H. Lee, J. D. Song, S. Stobbe, and P. Lodahl, Near-Unity Coupling Efficiency of a Quantum Emitter to a Photonic Crystal Waveguide, *Phys. Rev. Lett.* **113**, 093603 (2014).
- [31] F. T. Pedersen, Y. Wang, C. T. Olesen, S. Scholz, A. D. Wieck, A. Ludwig, M. C. Löbl, R. J. Warburton, L. Midolo, R. Uppu, and P. Lodahl, Near transform-limited quantum dot linewidths in a broadband photonic crystal waveguide, *ACS Photonics* **7**, 2343 (2020).
- [32] S. Mahmoodian, G. Calajó, D. E. Chang, K. Hammerer, and A. S. Sørensen, Dynamics of Many-Body Photon Bound States in Chiral Waveguide QED, *Phys. Rev. X* **10**, 031011 (2020).
- [33] O. A. Iversen and T. Pohl, Strongly Correlated States of Light and Repulsive Photons in Chiral Chains of Three-Level Quantum Emitters, *Phys. Rev. Lett.* **126**, 083605 (2021).
- [34] A. Carmele, N. Nemet, V. Canela, and S. Parkins, Pronounced non-markovian features in multiply Excited, multiple emitter waveguide QED: retardation induced anomalous population trapping, *Phys. Rev. Research* **2**, 013238 (2020).